JOURNAL OF AIRCRAFT
Vol. 32, No. 4, July–August 1995

Evaluation of Several Agility Metrics for Fighter Aircraft Using Optimal Trajectory Analysis

George W. Ryan III*
PRC Inc., Edwards, California 93523-0273
and
David R. Downing†
University of Kansas, Lawrence, Kansas 66044

This article presents the results from agility research performed under a grant through the University of Kansas. Several functional agility metrics, including the combat cycle time metric, dynamic speed turn plots, and relative energy state metric, are used to compare turning performance for generic F-18, X-29, and X-31-type aircraft models. These models are generic because they are 3-degree-of-freedom models that have characteristics similar to the real aircraft, but may not exactly represent the aircraft. The performance comparisons are made using data from optimal test trajectories to reduce sensitivities to different pilot input techniques and to reduce the effects of control system limiters. The turn performance for all three aircraft is calculated for simulated minimum time 180-deg heading captures from simulation data. Comparisons of the three aircraft give more insight into turn performance than would be available from traditional measures of performance. Using the optimal test technique yields significant performance improvements as measured by the metrics. These performance improvements were found without significant increases in turn radius.

Nomenclature

g = acceleration of gravity
h = altitude
M = Mach number
p = roll rate, deg/s
q = pitch rate, deg/s
V_c = corner velocity (velocity where max turn rate occurs)
V_T = total velocity of aircraft
X = acceleration due to forces in aircraft X direction
Y = acceleration due to forces in aircraft Y direction
Z = acceleration due to forces in aircraft Z direction
α = angle of attack, deg
β = angle of sideslip, deg
γ = flight-path angle
μ = flight-path bank angle
σ = flight-path heading angle
ϕ = payoff function

Introduction

THE standards of fighter aircraft performance analysis have changed as the technology in aircraft and weapon systems has evolved. For example, increased performance characteristics for modern fighters and the introduction of the all-aspect infrared (IR) missiles have prompted the development of several new fighter performance measures, called agility metrics. Most of these new measures concentrate on the transient capabilities of the aircraft, instead of the steady-state performance calculated by conventional performance standards. These agility metrics range from simple applications of combined steady-state performance measures to complicated mathematical derivations that measure agility potential. These metrics need to be applicable to any aircraft, independent of the type of aircraft or flight control system.

Presented as Paper 93-3646 at the AIAA Atmospheric Flight Mechanics Conference, Monterey, CA, Aug. 9–11, 1993; received April 5, 1994; revision received Dec. 30, 1994; accepted for publication Jan. 3, 1995.

*Aerospace Engineer, P.O. Box 273. Member AIAA.
†Chair, Aerospace Department. Associate Fellow AIAA.

Previous research[1] has shown that some agility metrics were sensitive to the test methods used to study them. The metrics that concentrate on maneuvers that last more than a few seconds can be greatly influenced by the methods used to test them and by the flight control system on the aircraft being tested. The combat cycle time (CCT) metric, the dynamic speed turn (DST) plots, and the relative energy state (RES) metric are examples of metrics sensitive to test procedures. It is desirable then to develop test methods that eliminate bias toward one type of aircraft or flight control system and to develop test techniques that eliminate errors caused by differences in pilot technique.

One way to develop these test methods is to use an optimal test trajectory. By using an optimal trajectory analysis program, maneuvers can be developed to exploit the maximum performance of each test aircraft for a given task. In this way, the comparisons of the aircraft reflect the maximum performance of each plane, not the abilities of the test pilot.

Agility Metrics Analyzed

The CCT[2] agility metric measures the time it takes for an aircraft to turn through a specified heading angle and regain the energy lost during the turn. The metric relates a combat-relevant task to a measure of time that is useful to pilots. This metric can be thought of as the time it takes to cycle around the limits of the turn rate vs Mach number plot, or "doghouse" plot, shown in Fig. 1. The times involved with the CCT metric include the following:

t_1 = time to roll 90 deg and load up to maximum normal load factor
t_{21} = time to reach corner speed, or the maximum turn rate
t_{22} = time to reach the new heading angle
t_3 = time to unload to a 1-g normal load factor and roll out
t_4 = time to accelerate back to the original energy level

The CCT is the sum of these times

$$\text{CCT} = t_1 + t_{21} + t_{22} + t_3 + t_4 \tag{1}$$

The goal is to achieve the lowest CCT possible.

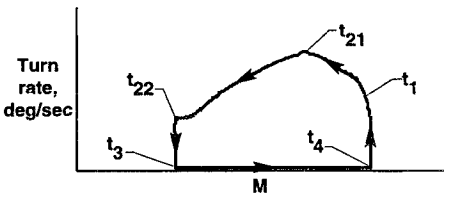

Fig. 1 Conceptual plot of CCT metric.

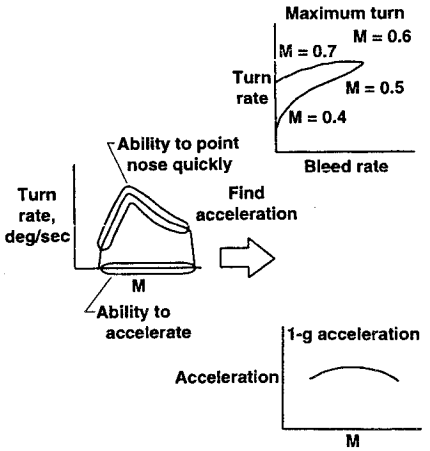

Fig. 2 Development of DST plots.

Though maneuver time is an important consideration for combat effectiveness, measuring the transient energy level during a maneuver is equally important. One metric that measures transient energy levels is the DST.[3] The DST plots relate energy state rate of change to spatial state rate of change. Cross-plotting the load factor and lift limit lines of the doghouse plot and the 1-*g* acceleration line along the bottom of the doghouse creates two plots. Figure 2 shows the conceptual development of these plots. The two plots on the right of Fig. 2 are derived from the plot on the left of the figure. The first derived plot, turn rate vs velocity bleed rate, is produced by measuring the turn rate and bleed rate at each point along the turning portion of the doghouse plot. Points along the load factor limit line and the lift limit line represent the turning potential of the aircraft. The second derived plot is obtained by taking points along the bottom of the doghouse to determine the 1-*g* acceleration capability of the aircraft.

These plots can be used to compare two aircraft to see which has superior acceleration capabilities, or to compare maneuvers for the same aircraft to see where increases in bleed rates do not yield significant increases in turn rate. The plots add another tool to the traditional energy maneuverability (EM) approach of analyzing aircraft performance by studying acceleration and deceleration. This time differentiation of traditional EM analysis techniques exposes differences between the efficiency of different maneuvers or aircraft because the transient maneuver is looked at instead of a steady-state condition.

Since aerial combat is not always a first-shot-only phenomenon, it is important to maintain maneuvering capabilities after the state of the aircraft has been changed during an initial defensive or offensive maneuver. For instance, the pilot can turn the flight path of an aircraft to a new heading angle and continue turning if necessary. This capability is needed to get a first-shot opportunity, to maneuver for a second shot or defensive maneuver, and to accelerate quickly to leave the engagement or attack another aircraft. However, engagement studies have revealed that fighters designed on the basis of superior first-shot performance alone may have unacceptable levels of energy loss, which results in degraded maneuverability. Therefore, a metric is needed that can measure turning capability while taking energy into account. The RES[3] is such a metric and is shown in Fig. 3.

The RES metric is a measure of the velocity of the aircraft relative to the corner speed of the aircraft. The ratio of aircraft velocity during the maneuver to the corner velocity of the aircraft (V/V_c) is plotted as a function of flight-path heading change. The plot shows how the aircraft turns its flight path while flying a certain control strategy. The point at which the line on the plot crosses the $V/V_c = 1$ line is where the aircraft has lost its ability to turn at high turn rates because the available energy has been depleted.

Analysis Method

The purpose of this analysis is to test the turn performance of the three aircraft of interest by using an optimal CCT test maneuver and to compare this turn performance using the functional agility metrics presented in the previous section. Functional agility metrics offer more insight into the turn performance of each aircraft than is available from traditional measures of performance.

For example, Fig. 4 shows a typical turn rate vs Mach number plot for the three aircraft. This plot is traditionally used to indicate the maximum turning capability of a given aircraft and to compare different aircraft. The plot contains lines representing the combination of Mach number and turn rate where the maximum lift for each aircraft is reached. An aircraft without poststall maneuvering capabilities cannot operate to the left of its maximum lift line in a sustained flight condition because the wing would be stalled. Figure 4 also contains a line representing the maximum normal load factor achievable for each aircraft at a given combination of turn rate and Mach number. For the three test aircraft, a normal load factor of 7.0 times the force of gravity is assumed to make the comparisons between the three models more equal. Any flight condition above the maximum normal load factor line for each aircraft could cause structural damage to the aircraft.

From the doghouse plot in Fig. 4, it appears that the F-18 has the best turn performance of 19 deg/s turn rate at a corner

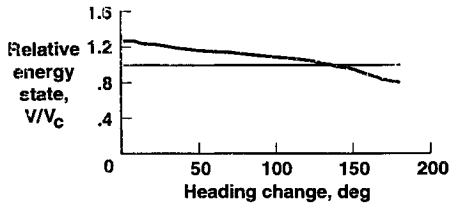

Fig. 3 Relative energy state concept plot.

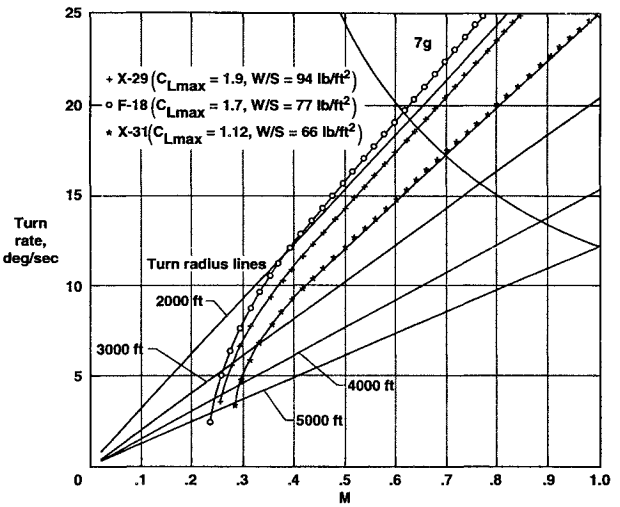

Fig. 4 Doghouse plot for test aircraft at 15,000 ft.

velocity of Mach 0.62. This is caused by a combination of a somewhat low wing loading of about 77 lb/ft^2 and a relatively high maximum lift coefficient of 1.7. The X-31 has a maximum turn rate of 17 deg/s at a corner velocity of about Mach 0.7. This is lower than the F-18 because of a lower maximum lift coefficient, despite having a lower wing loading of about 66 lb/ft^2. In contrast, the X-29 has a maximum lift coefficient of 1.9 and a maximum turn rate of about 18 deg/s at a corner velocity of approximately Mach 0.64. It also has a wing loading of about 94 lb/ft^2.

According to the doghouse plot, the aircraft would rank in the order of F-18, X-29, and X-31 when comparing maximum turn rate. This study will determine if the functional metrics introduced earlier rank the aircraft according to this order, or if they reveal information about each aircraft that is not available from the doghouse plot.

Previous analysis of these functional agility metrics has shown that the metrics are sensitive to the control strategy used to test them. For example, if the CCT metric is tested using maximum aft stick deflection during the turning portion of the maneuver, an aircraft with angle-of-attack (AOA) limiters in the flight control system will have a superior CCT by avoiding high AOA, high-induced-drag flight conditions.[4] Staying at a lower AOA reduces the energy lost during the maneuver, which in turn reduces the time needed to regain lost energy. This sensitivity to control inputs indicates that an optimal control strategy exists that would maximize the performance of a given airframe-flight control combination.

To verify this, optimal control strategies were calculated for the CCT maneuver using the optimal trajectories by implicit simulation (OTIS) program. The program was written by the Boeing Aerospace and Electronics Co., Seattle, Washington, under contract to the Wright Research and Development Center at the Wright–Patterson Air Force Base. It combines explicit and implicit integration techniques for optimizing a given scalar quantity. Details of the mathematical methods used are available in Ref. 5.

Optimal Trajectory Details

Solutions are sought to the following set of differential state constraints. The constraint equations are the equations of motion for the aircraft:

$$\frac{dx}{dt} = f(x, u, t) \tag{2}$$

where x corresponds to the aircraft states and u corresponds to the aircraft controls.

In addition to the differential state constraints, there also may be auxiliary variables, such as dynamic pressure, defined as

$$y = g(x, t) \tag{3}$$

The possible solutions to these equations must also satisfy path constraints of the form

$$\min^c \leq \begin{Bmatrix} x(t) \\ y(t) \end{Bmatrix} \leq \max^c \tag{4}$$

where $\min^c$ and $\max^c$ represent minimum and maximum values for the states and control variable values. Also, beginning and ending boundary values are imposed on the trajectory that must also be satisfied by the possible solution. They are written as

$$\min^{bc}(x, u) \leq B(x, u, t) \leq \max(x, u)^{bc} \tag{5}$$

where $\min^{bc}$ and $\max^{bc}$ represent the lower and upper boundary conditions to be satisfied, and B represents the boundary values for the states and controls.

The optimal solution to Eqs. 2–5 is defined as the set of vector time histories $x(t)$ and $u(t)$ that satisfies Eqs. (2–5) and minimizes the payoff function, $J(\phi)$, defined as follows:

$$J(\Phi) = \Phi(x, u) \tag{6}$$

This payoff, or cost function, represents a performance index to be minimized that is a function of the states and controls.

For the optimal trajectories found in this study, the previous equations can be represented by the following expressions.

The equations of motion for the aircraft are 3-degree-of-freedom (DOF) dynamic equations and are as follows:

$$\begin{aligned}
\dot{\sigma} &= (1/V_T \cos\gamma) + [-X(\cos\alpha \sin\beta \cos\mu \\
&\quad - \sin\alpha \sin\mu) + Y(\cos\beta \cos\mu) \\
&\quad - Z(\sin\alpha \sin\beta \cos\mu + \cos\alpha \sin\mu)] \\
\dot{\gamma} &= (1/V_T)[X(\cos\alpha \sin\beta \sin\mu \\
&\quad + \sin\alpha \cos\mu) - Y(\cos\beta \sin\mu) \\
&\quad + Z(\sin\alpha \sin\beta \sin\mu - \cos\alpha \cos\mu) - g\cos\gamma] \\
\dot{V}_T &= [X(\cos\alpha \cos\beta) + Y(\sin\beta) \\
&\quad + Z(\sin\alpha \cos\beta) - g\sin\gamma]
\end{aligned} \tag{7}$$

The auxiliary variables of interest are not included in the optimization procedure, and so Eq. (3) is not included in the analysis. The auxiliary variables include parameters such as turn radius and turn rate. The path constraints for this problem are defined as

Angle of attack

$$-10 \leq \alpha \leq 60 \text{ deg for F-18}$$
$$-10 \leq \alpha \leq 70 \text{ deg for X-31}$$
$$-10 \leq \alpha \leq 60 \text{ deg for X-29}$$

Angle of sideslip

$$-0 \leq \beta \leq 0 \text{ deg}$$

Roll angle

$$-180 \leq \phi \leq 180 \text{ deg}$$

Throttle

$$\text{Flight idle to maximum } A/B$$

Normal acceleration

$$-3 \leq n_z \leq 7.0\ g \text{ for all three aircraft}$$

Altitude

$$13{,}500 \leq h \leq 16{,}500 \text{ during turn}$$
$$h_f = \text{altitude at end of turn } \pm 200 \text{ ft}$$

Angle-of-attack rate

$$-30 \leq \dot{\alpha} \leq 30 \text{ deg/s for F-18}$$
$$-25 \leq \dot{\alpha} \leq 25 \text{ deg/s for X-31}$$
$$-20 \leq \dot{\alpha} \leq 20 \text{ deg/s for X-29}$$

Bank angle

$$-120 \leq \dot{\mu} \leq 120 \text{ deg/s for F-18}$$

$$-130 \leq \dot{\mu} \leq 130 \text{ deg/s for X-31}$$

$$-120 \leq \dot{\mu} \leq 120 \text{ deg/s for X-29}$$

Final heading

$$180 \text{ deg} \pm 2 \text{ deg}$$

With these path constraints for the possible solutions, the following initial and final boundary conditions were placed on the trajectories:

Initial conditions

$$\text{Mach 0.8 initial velocity} = M_0$$

$$\text{15,000-ft initial altitude} = h_0$$

$$\text{0-deg initial heading} = \psi_0$$

Final conditions

$$\text{Mach 0.8 final velocity} = M_0$$

$$\text{180-deg final heading} = \psi_f$$

These limits and constraints are added into the optimization problem by adjoining them to the cost function through multipliers. The cost function for this study is a simple time function, since the main objective for analyzing the CCT maneuver is to reduce the total maneuver time. Therefore, the objective function is

$$J = \int_{t_1}^{t_4} dt \tag{8}$$

The resulting two-point boundary value problem is solved by the OTIS program using a sequential-nonlinear quadratic programming (SNLQP) method after calculating a quadratic approximation to the objective function. A review of standard sequential quadratic programming methods is available in Ref. 6.

Aero and propulsion data for a full 3-DOF simulation of each aircraft being studied are used inside the program to simulate the systems. The data for the test aircraft models were collected from nonlinear simulations, and have been compared to 6-DOF models for accuracy. The weights used in the simulations for the F-18, X-31, and X-29 were 30,890, 14,700, and 17,430 lb, respectively. These amounts represent the weight of each aircraft with 20% of the empty weight added as fuel weight. This fuel weight was chosen as a fraction of the empty weight to standardize the test weights used.

The test conditions for the maneuvers consisted of an initial altitude of 15,000 ft and an initial Mach number of 0.8. Using the test weights with the input aerodynamic and propulsion models for each aircraft, optimal trajectories for minimum time 180-deg heading captures were calculated. The optimization included a level acceleration segment to allow the aircraft to accelerate back to the energy level present before the turn was started. The optimal trajectories were calculated with realistic limitations on the aircraft states, such as normal load factor, roll rate μ, and pitch rate θ. The normal load factor limit used for the F-18, X-31, and X-29 was 7.0 g. This limit is displayed in Fig. 4 and represents a value obtainable for fighter-type aircraft. Standardizing the normal load factor limit for all three aircraft made comparisons easier.

The resulting optimal trajectories included optimal schedules for angle of attack α and bank angle μ. The angle-of-attack time histories calculated by OTIS are shown in Fig. 5,

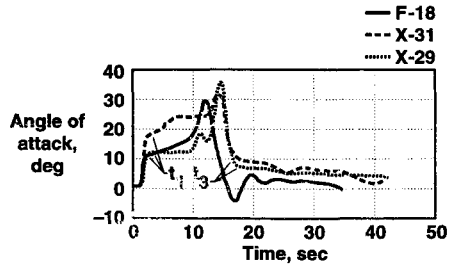

Fig. 5 AOA time history.

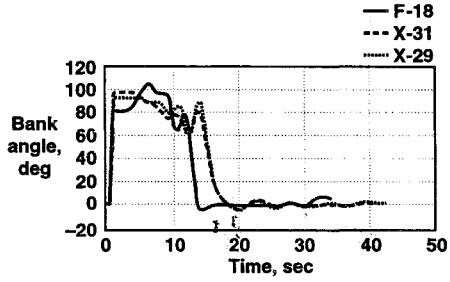

Fig. 6 Bank angle time history.

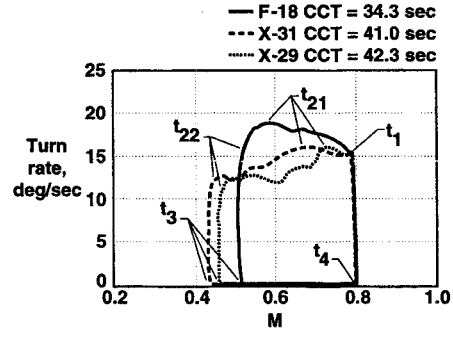

Fig. 7 Combat cycle time results.

with the optimal bank angle time histories shown in Fig. 6. Figure 5 also shows the point during each maneuver where each aircraft reached maximum normal load factor and unloaded from the turn at t_1 and t_3, respectively. The data generated from these maneuvers were then used to calculate the agility metrics to be analyzed. The constraints placed on the altitude and the final energy state resulted in optimal trajectories that are not high-AOA maneuvers. This is because the acceleration phase and altitude limits penalize high-AOA maneuvers that result in large energy losses and increased maneuver times.

Combat Cycle Time Results

Figure 7 shows the resulting CCT plots for the three test aircraft and illustrates differences and similarities in aircraft performance. These plots reflect the maximum available turning performance for the three aircraft, while still allowing for a minimum time acceleration phase at the end of the turn. The time point flags included on the plot show where the time segments are finished for each aircraft. Table 1 contains the time values between segments from the CCT maneuvers.

The CCT for the F-18 in Fig. 7 shows that the F-18 can roll into the turn and pitch up to maximum normal load factor in only 2.4 s, or t_1 as shown in the table and in Fig. 5. The normal load factor time history is shown in Fig. 8. The initial turning portion of the maneuver, up to time t_{21}, shows that the F-18 turns along the maximum normal load factor limit line until it reaches a maximum turn rate of about 18 deg/s. The F-18 reaches its maximum turn rate near its corner velocity of about Mach 0.62. By flying the F-18 at a high average turn rate, the

Table 1 Combat cycle time results for test cases

Test case, optimal CCT	t_1	t_{21}	t_{22}	t_3	t_4	Total CCT, s
F-18	2.4	8.9	2.2	1.4	19.4	34.3
X-31	2.6	3.5	9.1	1.8	24.0	41.0
X-29	3.0	3.4	9.3	1.5	25.1	42.3

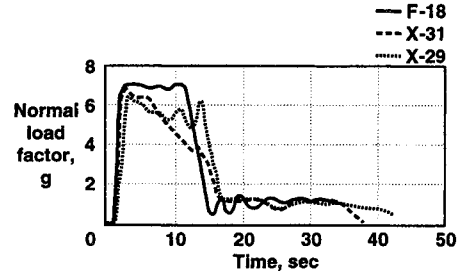

Fig. 8 Normal load factor plot.

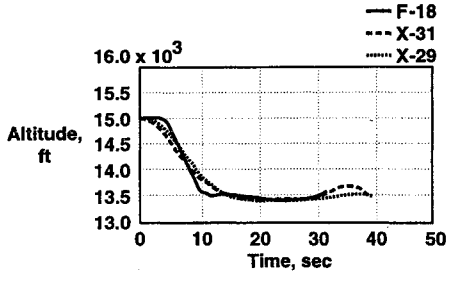

Fig. 9 Altitude plot for turn maneuvers.

180-deg heading change only takes 13.5 s. This is indicated by time segments t_1 to t_{22}. Figure 9 shows that during the turn, the F-18 uses all available altitude, since the lower limit was set to 13,500 ft. Next, the F-18 unloads to a 1-g level flight condition and begins to accelerate. The time to unload and roll out is only 1.4 s, or t_3, whereas the time to accelerate back to the original energy level is 19.4 s, or t_4. Figure 9 shows that during the acceleration, the F-18 uses the ±200-ft limit while it accelerates. The result of adding the maneuver segments together is a total CCT of 34.3 s. This is a 20% reduction in total maneuver time when compared to previous values of this metric. To compare these figures, Ref. 1 contains results calculated for the F-18 using a standard full-aft-stick test strategy.

The CCT for the X-31 aircraft is slightly greater than that of the F-18. The time needed to roll and pitch up to maximum normal load factor is only 2.6 s. This maximum normal load factor is shown in Fig. 8. The time needed to turn to the new heading angle is slightly greater than that of the F-18, at 15.2 s from adding t_1, t_{21}, and t_{22}. This increased turn time over the F-18 is caused by the lower maximum lift coefficient of the X-31 and the fact that the F-18 stays at a higher turn rate throughout the turn. The maximum turn rate during the turn, achieved at time t_{21}, is about 16 deg/s at a corner velocity of Mach 0.7. Figure 8 shows that the X-31 also takes advantage of the available altitude to stay near corner velocity during the turn. Next, the time needed to unload and roll out of the turn (t_3) is 1.8 s. The X-31 takes much more time (24.0 s) to regain its original energy level. This is because of the lower velocity at which the X-31 completes the turning portion of the maneuver. Figure 9 shows that the X-31 also takes advantage of the ±200-ft change in altitude limit during the acceleration to help unload and reduce the drag by reducing AOA at the beginning of the acceleration. The total CCT for the X-31 is 41.0 s. This is a 20% time increase over the F-18. This increase is caused by the lower conventional turning performance of the X-31 when compared to the F-18, caused by a lower maximum available lift coefficient. Figure 10 shows that the X-31 turns at a larger turn radius than the F-18.

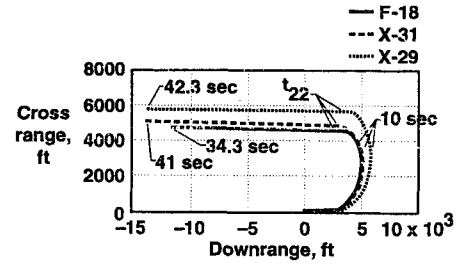

Fig. 10 Downrange and cross range for the turn maneuvers.

The CCT plot for the X-29 is similar to the other two aircraft. The time needed to roll and load up to maximum load factor is only slightly increased, at 3.0 s for t_1. Figure 8 shows that the X-29 loads up to just below the limit by rolling into the turn and increasing AOA, similar to the other aircraft. However, the plot in Fig. 7 shows that the X-29 turns at a low average turn rate when compared to the other two aircraft. By holding the X-29 to this lower average turn rate, the optimal trajectory avoids high-AOA conditions that would cause large energy losses. The X-29 turns to the new heading in only 15.7 s and reaches a maximum AOA of only 35 deg. This is slightly higher than the maximum AOA (approximately 30 deg) of the other two aircraft. The AOA where the X-29 has its highest lift coefficient is about 40 deg, indicating that the optimal trajectory has the X-29 preserve energy by staying below $C_{L\max}$. Figure 9 shows that the X-29 also uses the available altitude to maintain a high energy level during the turn. After the X-29 unloads to a 1-g condition and rolls out of the turn, it takes 25.1 s to regain the lost energy. This performance is similar to that of the X-31 and 29% greater than that of the F-18. The total maneuver time of 42.3 s is a 5% reduction when compared to values of this metric found in previous research for the X-29.[4]

Comparing the different time segments of the three CCT plots illustrates the differences between the aircraft. The F-18 turns at a relatively low AOA at the start of the turn, with a quick pitch excursion at the end of the turn to capture the desired heading to about 30-deg AOA. The X-31 turns at a low AOA below corner velocity, increases AOA slightly as velocity is bled off, and uses a similar pitch excursion to about 32-deg AOA to capture the new heading. The maximum lift coefficient for the X-31 occurs at about 30 deg. In contrast, the X-29 uses a pitch excursion to about 35-deg AOA toward the end of the turn, which is higher than the other two aircraft. This is because the maximum available lift coefficient occurs at an AOA of about 40 deg, which is where the X-29 should have its maximum turning capability at low speeds. The AOA time history indicates that the optimization routine causes the aircraft to turn to within a few degrees of the desired heading at lower AOA and then to use a quick excursion to slightly below $C_{L\max}$ to capture the final heading. This AOA increase at the end of the turn is consistent with newer turn performance test techniques used to flight test agility characteristics.[7]

The results of the CCT analysis indicate that this metric gives some insight into how quickly the aircraft can move from one maneuver state to another. Though this metric is dominated by traditional measures, such as maximum turn rate and thrust-to-weight ratio, it is useful for looking into how quickly an aircraft can perform a combat-relevant task. This metric shows that the F-18 has superior turn performance over the other aircraft, which is consistent with the information given in the doghouse plot in Fig. 4.

DST Plot Results

The DST plots were also calculated using the data from the minimum time heading captures for each aircraft. The first

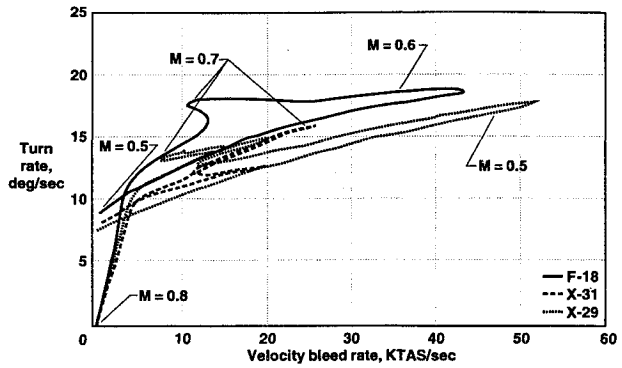

Fig. 11 Velocity bleed rate DST plot.

of the DST plots (Fig. 11) shows how efficiently each aircraft can turn. The aircraft with the maximum velocity bleed rate is the least efficient, trading large amounts of energy to achieve a small turn radius. In contrast, the aircraft with the lowest velocity bleed rate turns without expending too much of its total energy. The flags indicating Mach number during the maneuver are included to give more information for the aircraft velocity during the maneuver, which begins at the lower left of the plot in Fig. 11.

Figure 11 shows that the F-18 decelerates as it turns and reaches a maximum velocity bleed rate of about 43 knots true airspeed (KTAS)/s at an airspeed of Mach 0.6. This is a reduction of about 30% when compared to the 60 KTAS/s bleed rate values for the same maneuver found in previous research.[1] This reduction in maximum bleed rate is caused by a 45% reduction of the maximum AOA achieved during the maneuver when compared to the previous results. Instead of pulling and holding full-aft stick through the turn, as was done in previous tests,[4] the optimal maneuver AOA was used. After the turn is completed and the aircraft begins to accelerate, it is left with a reserve turn rate of almost 10 deg/s. This is indicated by the point where the line for the F-18 touches the left side of the plot after the turn is complete. This would allow the F-18 to continue to maneuver effectively after making the 180-deg heading change to acquire the enemy.

The X-31 decelerates the turn similar to the F-18, reaching its maximum velocity bleed rate at about Mach 0.7. However, the X-31 has a lower maximum velocity bleed rate during the turn, which shows that it loses energy at a slower rate than the F-18. This was also seen from the CCT results because the X-31 was moving at a lower turn rate and lift condition than the F-18, which indicates a lower drag condition. The maximum bleed rate is about 25 KTAS/s, which is almost 50% lower than that of the F-18. Also, the residual turn rate for the X-31 is slightly lower than that of the F-18, at about 8 deg/s. However, this would still allow the X-31 to continue maneuvering to acquire a target after the 180-deg turn.

The plot for the X-29 shows that the aircraft exchanges velocity for increased turn rates toward the end of the turn. The slope of the line in Fig. 11 for the X-29 when it is at about Mach 0.5 shows that the increased velocity bleed rates are not yielding significant increases in turn rate. However, the X-29 does not stay at these high bleed rates for a long time, because they occur during the final stick pull at the end of the turn to capture the final heading. This short duration indicates that only a small amount of velocity is lost by going to these high bleed rates. Figure 11 also shows that the residual turn rate for the X-29 after the 180-deg heading change is lower than that of the X-31 or the F-18 at about 7 deg/s.

Figure 12 contains the level acceleration plot of the DST plots. This figure shows that the three aircraft accelerate at similar rates while in level flight. The F-18 accelerates at an average rate of about 9 KTAS/s, indicating that regaining the velocity loss of approximately 180 KTAS from the 180-deg turn should take about 20 s. This is consistent with the CCT results for the F-18.

Similarly, Fig. 12 also shows that the maximum acceleration rate of the X-31 is similar to that of the F-18, at 9 KTAS/s. This indicates that the velocity loss of about 220 KTAS during the turn should take about 24 s to regain. This is also consistent with previous results for the X-31. This level acceleration rate indicates that the F-18 and X-31 have similar thrust-to-weight ratios.

The X-29 can accelerate at a level rate of about 9 KTAS/s, which is similar to the F-18 and X-31. This shows that the X-29 should be able to regain airspeed as quickly as the F-18. However, since the X-29 is accelerating from a lower initial velocity, the acceleration phase takes longer. The 230-KTAS velocity loss should take about 25 s to regain, which is consistent with the acceleration phase results of the CCT metric.

Comparing the results for the DST plots gives some insight into the turn performance of the three aircraft that is not available from standard performance measures. For example, the residual turn rate after the 180-deg turn for the three aircraft indicates that the F-18 continues to maneuver with a higher turn rate than the other aircraft. In addition, the acceleration plot shows that despite having different configurations, the three aircraft accelerate in level flight at about the same rate if all three aircraft start from a low AOA.

RES Results

The RES was calculated for each aircraft during the 180-deg heading change (Fig. 13). This plot shows the energy efficiency of each aircraft as it turns through the desired heading angle. The initial RES for the aircraft vary because of the difference in corner velocity for each aircraft. At 15,000 ft, the F-18 has a corner velocity at about Mach 0.62, as shown in Fig. 4. At the same condition, the X-31 and the X-29 corner velocities are Mach 0.7 and Mach 0.64, respectively.

The line representing the RES of the F-18 shows that the aircraft can turn through about 130 deg of heading before it has depleted its velocity to a level below corner speed. The RES plot indicates that the ability of the pilot to turn at high turn rate values is not reduced until after the F-18 turns through 130 deg.

In contrast, the X-31 aircraft can only turn through approximately 40 deg before the RES goes below $V/V_c = 1$. The turn rate capability of the X-31 is not as high as the F-18 in this maneuver. However, since the X-31 was designed to bleed velocity quickly to enter poststall maneuvers, this

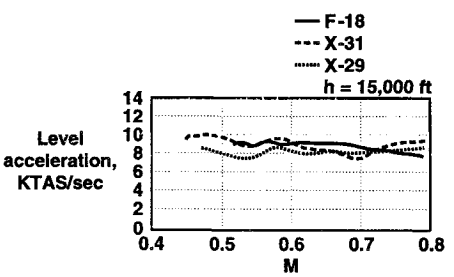

Fig. 12 Figure level acceleration plot for test aircraft.

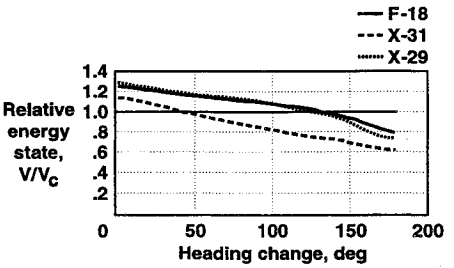

Fig. 13 Comparison of relative energy states.

was expected. Also, since the corner velocity of the X-31 is high because of a somewhat low maximum lift coefficient, a small loss in velocity quickly puts the aircraft below corner velocity. This is a clear indication of the different design philosophies behind the F-18 and X-31.

The relatively high maximum lift coefficient of the X-29 gives it a corner velocity similar to that of the F-18, even though it has a significantly higher wing loading than the F-18. The X-29 has an efficient forward-swept wing, with a relatively high aspect ratio with the main surfaces lifting in this flight condition. Figure 13 shows that the X-29 can turn through almost 130 deg before losing significant energy. The static instability of the aircraft allows the canard and the wing to contribute positive lift in the turn, reducing the lift lost to trimming the aircraft.

This metric gives the designer or engineer insight into the efficiency of each aircraft as it turns. The plot indicates that the X-29 is more efficient at the initial heading changes, because of a superior lift-to-drag ratio. However, as the aircraft turns farther, the X-29 loses energy quickly at high AOA and its RES decreases to a value similar to the F-18. The X-31 can only turn through a small heading change before it has bled off speed to a level significantly below corner velocity.

Conclusions and Recommendations

The calculation of the previously mentioned metrics using the optimal test maneuver indicates that information is available from these metrics that would not be available from standard measures of merit. Also, performance improvements can be realized if the optimal test maneuvers are used to calculate the metrics, rather than the standard procedures previously used in flight tests.

The combat cycle time combines combat-relevant tasks into a single time value, although the metric is dominated by the standard measures of merit of sustained turning performance and thrust-to-weight ratio. This makes comparisons between aircraft simple, and shows how well an aircraft can move between maneuver states. According to the combat cycle time metric, the F-18 has superior performance over the other two test aircraft, despite the superior maximum lift coefficient for the X-29. Because the three aircraft use the available altitude set by the constraints on the optimization during the turn, it would be interesting to note the effect of removing or expanding the limits of this constraint.

The dynamic speed turn plots are calculated using the data from the minimum time heading captures for each aircraft. This metric measures the transient energy management capabilities of an aircraft for a given task and provides easy comparison of different aircraft. Comparisons are simple because maximum energy bleed rate and maximum acceleration capabilities are measured. According to this metric, the X-31 has superior energy management capabilities because it can turn without reaching velocity bleed rate values as high as the other aircraft. It can also regain lost velocity with an acceptable level acceleration capability compared to the other aircraft.

The relative energy state metric measures how quickly an aircraft turns and how well it maintains velocity during the turn close to corner velocity. It also measures the turning efficiency of an aircraft, and compares the maximum heading change that an aircraft is capable of before it needs to stop turning and accelerate to regain energy. According to this metric, the F-18 and X-29 are able to turn through greater heading changes than the X-31 before velocity decreases below corner velocity.

The following is a list of performance improvements available for the values of these metrics by using an optimal test maneuver.

1) The F-18 combat cycle time can be reduced by 20% without significant increases in the turning radius for a 180-deg heading capture.

2) The X-29 combat cycle time can be reduced by 5% without increases in turn radius by following the optimal test maneuver.

3) The maximum velocity bleed rate and the maximum angle of attack can be reduced by 30 and 45%, respectively, for the F-18 aircraft if an optimal test schedule is used, rather than the typical test technique.

The following recommendations are made as a result of the tests performed for this study.

1) Although the metrics provide a glimpse of the performance capabilities of the test aircraft used in this study, they must be applied with great care to ensure that comparisons are not biased toward an aircraft. Optimization of a given task is one way to ensure each aircraft is performing at its maximum capability.

2) These metrics, representing maneuvers that take several seconds to perform, are sensitive to the test methods used to evaluate them. This may not make them suitable for flight test, since repeatability is an issue.

3) This study looked at only one type of maneuver, and should be extended to include other types of maneuvers, such as turns through different heading angles, and turns at different turn radii. Also, it would be interesting to vary aircraft configuration parameters, such as wing loading, maximum lift coefficient, and maximum normal load factor.

4) The addition of the acceleration phase into the optimization problem prohibits the aircraft from flying at high AOA conditions to avoid large energy losses. This subsequently excludes poststall maneuvers from the possible solutions. It would be interesting to expand this technique to include poststall supermaneuvers. Research has indicated that this type of maneuver can result in quick heading changes with small turn radius values at the expense of large energy losses.

5) The data presented here are for the generic models generated from simulator data, and may not reflect the data from a flight test study of these aircraft. It would be interesting to perform these maneuvers in a flight test environment to see if they show the same trends.

6) The agility metrics used in this analysis, and the other existing metrics, need to be tested against exchange ratios from flight data and simulation studies. This would allow conclusions to be drawn between combat effectiveness and a certain metric value.

Acknowledgments

The research in this article was made possible by the support of the NASA Dryden Flight Research Center through Cooperative Agreement NCC-2-588 and Contract NAS2-13445. This support was greatly appreciated and a note of thanks is extended to all those involved with the research at NASA Dryden and the University of Kansas.

References

[1]Ryan, G. W., III, and Downing, D. R., "The Evaluation of Several Functional Fighter Agility Metrics Using Optimal Trajectory Analysis Techniques," AIAA Paper 92-4488, Aug. 1992.

[2]Tamrat, B. F., "Fighter Aircraft Agility Assessment Concepts and Their Implication on Future Agile Aircraft Design," AIAA Paper 88-4400, Sept. 1988.

[3]McAtee, T. P., "Agility—Its Nature and Need in the 1990's," Society of Experimental Test Pilots Symposium, Beverly Hills, CA, Sept. 1987.

[4]Cox, B., "Evaluation of Several Functional Fighter Agility Metrics for Fighter Class Aircraft," M.S. Thesis, Univ. of Kansas Aerospace Engineering Dept., Lawrence, KS, Aug. 1991.

[5]Hargraves, C. R., and Paris, S. W., "Direct Trajectory Optimization Using Nonlinear Programming and Collocation," *Journal of Guidance, Control, and Dynamics*, Vol. 10, No. 4, pp. 338–342.

[6]Gill, P. E., Murray, W., and Wright, M., *Practical Optimization*, Academic, San Diego, CA, 1981.

[7]Butts, S. L., and Lawless, A. R., "Flight Testing for Aircraft Agility," AIAA Paper 90-1308, May 1990.